

Title:

Electrical transport and magnetic properties of $\text{Mn}_3\text{O}_4\text{-La}_{0.7}\text{Ca}_{0.3}\text{MnO}_3$ ceramic composites prepared by a one-step spray-drying technique

Authors:

B. Vertruyen^{a,*}, J.-F. Fagnard^b, Ph. Vanderbemden^b, M. Ausloos^c, A. Rulmont^a, R. Cloots^a

^a SUPRATECS/LCIS, Chemistry Institute B6, University of Liege, Sart-Tilman, B-4000 Liège, Belgium

^b SUPRATECS, Department of Electrical Engineering and Computer Science B28, University of Liege, Sart-Tilman, B-4000 Liège, Belgium

^c SUPRATECS, Physics Institute B5, University of Liege, Sart-Tilman, B-4000 Liège, Belgium

* Corresponding author:

e-mail: b.vertruyen@ulg.ac.be, phone : + 32 4 3663452, fax : + 32 4 3663413

Abstract

$\text{La}_{0.7}\text{Ca}_{0.3}\text{MnO}_3/\text{Mn}_3\text{O}_4$ composites can be synthesized in one step by thermal treatment of a spray-dried precursor, instead of mixing pre-synthesized powders. Another advantage of this composite system is that a long sintering step can be used without leading to significant modification of the manganite composition. The percolation threshold is reached at ~20 vol% of manganite phase. The 77K low field magnetoresistance is enhanced to ~11% at 0.15 T when the composition is close to the percolation threshold.

Keywords:

Composites; Perovskites; Spray drying; Electrical properties

Introduction

The magnetoresistance properties of the perovskite manganite compounds $\text{La}_{1-x}\text{A}_x\text{MnO}_3$ (where A is an alkaline-earth cation) have recently attracted considerable research interest.¹ Intrinsic Colossal MagnetoResistance (CMR)¹ is observed when a rather large (>1T) magnetic field is applied to the material in the temperature range corresponding to the transition between a low-temperature metallic-ferromagnetic state and a high-temperature insulating-paramagnetic state. Polycrystalline samples display an additional extrinsic magnetoresistance effect, which is not as large as the CMR but is obtained for much smaller magnetic field (typically less than 0.2 T) and all temperatures below the transition temperature.² Several authors³⁻⁹ have tried to enhance this low field magnetoresistance (LFMR) by mixing the manganite phase with an insulating phase. In order to prevent interdiffusion between the phases, these "composites" are submitted to very short sintering treatment (typically 1 hour).³⁻⁶ This results in a large porosity of the samples and a poor connectivity between the manganite grains. On the other hand, when long sintering times are used to reach proper densification, it is usually observed that the composition and properties of the manganite phase are drastically modified due to interdiffusion between the phases.⁷⁻⁹

The present paper reports the synthesis and properties of a composite system that can be submitted to long sintering treatment without leading to significant modification of the manganite composition: these unique properties of the $\text{La}_{0.7}\text{Ca}_{0.3}\text{MnO}_3/\text{Mn}_3\text{O}_4$ system result from the fact that no compound with $\text{Mn}/(\text{La}+\text{Ca}) > 1$ exists in the composition, temperature

and pressure ranges used during the synthesis of the composite samples.¹⁰ An additional advantage of this system is the possibility to synthesize the composite samples in one step by thermal treatment of a spray-dried precursor, instead of mixing pre-synthesized manganite and insulating powders.

Experimental

Samples with nominal composition " $\text{La}_{0.7}\text{Ca}_{0.3}\text{MnO}_3 + n \text{MnO}_z$ " ($0 \leq n \leq 7$) were synthesized by thermal treatment of precursor powders prepared by the spray drying technique.¹¹ The aqueous feedstock solution was prepared by dissolving in water stoichiometric amounts of lanthanum acetate and calcium acetate whose exact stoichiometry had been determined by thermogravimetric analysis. For each sample, an appropriate amount of manganese acetate was added to a known volume of the lanthanum and calcium solution. The final concentration $[\text{La}^{3+} + \text{Ca}^{2+} + \text{Mn}^{2+}]$ was in the 0.4-0.8 mol/l range.

Spray drying was performed through a co-current flow atomisation process in a Büchi B-191 apparatus using a 0.7 mm nozzle. The inlet temperature was 200°C. The liquid feed rate was 1.4 ml/min. The spray drying was carried out in air, using a flow rate of 600 normal l/h. The outlet temperature during spraying was 140-145°C.

After spray drying, each powder was heated in air at 600°C during 5h in alumina crucibles. A slow heating rate (10°C/h) was used in the 200-350°C temperature range. After grinding, each powder was calcined at 900°C during 10 h. The powders were then pressed uniaxially into 13 mm diameter pellets and sintered in air at 1250°C during 12 h and 1300°C during 40 h.

Powder X-ray diffraction patterns were collected with a Siemens D5000 diffractometer ($\text{Cu K}\alpha$) and analysed with the Bruker TOPAS software. The morphology of the samples was studied by scanning electron microscopy (Philips XL30 FEG-ESEM). The cationic composition was checked by Energy Dispersive X-ray Analysis (EDAX system). The density of the pellets was measured by Archimedes' method in 1-butanol. The electrical and magnetic properties were measured as a function of temperature and magnetic field using a Quantum Design PPMS (Physical Property Measurement System) and a Keithley 617 Programmable Electrometer.

Results and discussion

In the following, samples with nominal composition " $\text{La}_{0.7}\text{Ca}_{0.3}\text{MnO}_3 + n \text{MnO}_y$ " ($0 \leq n \leq 7$) will be labelled Mn-#, where # = $n \cdot 100$ corresponds to the Mn excess, given as a percentage of the stoichiometric Mn amount in $\text{La}_{0.7}\text{Ca}_{0.3}\text{MnO}_3$.

Powder X-ray diffraction (XRD) patterns of all samples except Mn-0 reveal the presence of two phases: a perovskite phase with composition close to $\text{La}_{0.7}\text{Ca}_{0.3}\text{MnO}_3$ and a Mn_3O_4 phase. The cell parameters of the perovskite phase are not constant throughout the series but increase slightly when the Mn_3O_4 content increases. The cell volume data are plotted as a function of Mn excess in Figure 1. The crystallographic parameters of the single-phase manganite sample (Mn-0) and the sample Mn-700 agree well with literature values¹² for $\text{La}_{0.7}\text{Ca}_{0.3}\text{MnO}_3$ and $\text{La}_{0.72}\text{Ca}_{0.28}\text{MnO}_3$ respectively.

The study of polished cross-sections by electron microscopy and EDX analysis confirmed the XRD results. Figure 2 presents an electron micrograph for a representative sample, where the manganite phase and Mn_3O_4 phase appear in light and dark grey respectively. The porosity of the samples (measured by Archimedes' method) is less than 10% for Mn excess below 500% and progressively increases to ~25 % for the sample with the largest Mn_3O_4 content (Mn-700). That porosity was taken into account when calculating the manganite volume fraction values plotted in Figure 1.

The results of magnetic measurements are summarised in Figure 3. The Curie temperature T_C corresponding to the paramagnetic-ferromagnetic transition decreases slightly when the Mn excess is increased. This ~ 20 K decrease is very small when compared to the drastic drop usually observed in such composites as a result of interdiffusion between the manganite phase and the insulating phase⁷⁻⁹. This indicates that the composition of the manganite phase is almost constant throughout the series, as already observed by XRD. This is further corroborated by the inset of Figure 3, where the experimental values of the magnetization at 2T, 10K are in good agreement with a theoretical line calculated by considering that the composites are made up of mixtures of $\text{La}_{0.7}\text{Ca}_{0.3}\text{MnO}_3$ and Mn_3O_4 .

In $\text{La}_{0.7}\text{Ca}_{0.3}\text{MnO}_3$ -type manganites, the magnetic transition is usually coupled to a resistive transition between a metallic-like state at low temperature and an insulating-like state at high temperature.¹ The resistive transition temperature T_{IM} of the composites is shown in Figure 3. It agrees with T_C within a few degrees. However no resistive transition is observed when the Mn excess exceeds 633% (i.e. when the manganite volume fraction is smaller than $\sim 20\%$). Besides, the disappearance of the resistive transition is coupled to a dramatic increase of the electrical resistivity (more than 5 orders of magnitude), as shown in Figure 4 where the resistivity values at 300 K are plotted as a function of the manganite volume fraction. These phenomena correspond to the crossing of the percolation threshold, i.e. the disappearance of a continuous conductive path through the manganite phase. That $\sim 20\%$ value for the critical percolation volume fraction is close to the values predicted¹³ for three-dimensional continuum media from the theoretical results for various regular lattices: it has been shown that all usual 3D lattice types display a critical volume fraction Φ_c in the range $(16 \pm 2)\%$, where $\Phi_c = v P_{cs}$ with v the filling factor and P_{cs} the critical site occupation probability.¹³

Figure 5 shows the influence of a magnetic field on the electrical resistance of a sample with composition close to the percolation threshold (manganite volume fraction just larger than 20%). The data are presented as R/R_0 values, where R_0 is the electrical resistance in the hysteresis loop at $H=0$. The curve collected at 10 K displays a large hysteresis effect. Starting from the low-resistance state at positive magnetic field, the resistance increases when the magnetic field decreases and reaches a maximum value for a slightly negative field rather than at 0 T. When the field is scanned from negative to positive values, a similar dependence is observed, with a resistance peak occurring for a slightly positive magnetic field. This behaviour is common in manganite samples and several authors^{11,14} have shown that the resistivity maxima occur at fields corresponding to the coercive fields $+\mu_0 H_C$ and $-\mu_0 H_C$. In the present case, the main cause for the significant coercive field is the presence of Mn_3O_4 , which is ferrimagnetic and shows a strong magnetic irreversibility below 44 K. At 77 K, the hysteresis effect is much smaller, as shown in Figure 5 and the inset of Figure 4. The magnetoresistance effect ($\text{MR} = \{R/R_0\} - 1$) at 77 K reaches -11% at 0.15 T and -24% at 2T. The magnetoresistance close to room temperature (270 K) is smaller (-11% at 2T) and displays the parabolic-like $R(H)$ shape usually observed in manganite samples close to the transition temperature.¹ At all temperatures, the LFMR effect is significantly larger in the sample close to the percolation threshold than in the single-phase manganite sample, as observed by other authors in different composite systems.³⁻⁶

Conclusion

$\text{La}_{0.7}\text{Ca}_{0.3}\text{MnO}_3/\text{Mn}_3\text{O}_4$ composites were synthesized in one step by thermal treatment of a spray-dried precursor. A long sintering step was used without leading to significant modification of the manganite composition. The percolation threshold is reached at ~ 20 vol% of manganite phase. The 77K low field magnetoresistance is enhanced to $\sim 11\%$ at 0.15 T when the composition is close to the percolation threshold.

Acknowledgments

BV thanks the F.N.R.S. in Belgium for a Postdoctoral researcher fellowship. Part of this work was supported by the European Network of Excellence FAME.

References

1. Coey, J.M.D., Viret, M. & von Molnar, S., Mixed-valence manganites, *Adv. Phys.*, 1999, **48**, 167-293.
2. Ziese, M., Extrinsic magnetotransport phenomena in ferromagnetic oxides, *Rep. Prog. Phys.*, 2002, **65**, 143-249.
3. Petrov, D.K., Krusin-Elbaum, L., Sun, J.Z., Feild, C. & Duncombe, P.R., Enhanced magnetoresistance in sintered granular manganite/insulator systems, *Appl. Phys. Lett.*, 1999, **75**, 995-997.
4. Balcells, L., Carrillo, A.E., Martinez, B. & Fontcuberta, J., Enhanced field sensitivity close to percolation threshold in magnetoresistive $\text{La}_{2/3}\text{Sr}_{1/3}\text{MnO}_3/\text{CeO}_2$ composites, *Appl. Phys. Lett.*, 1999, **74**, 4014-4016.
5. Gupta, A., Ranijt, R., Mitra, C., Raychaudhuri, P. & Pinto, R., Enhanced room-temperature magnetoresistance in $\text{La}_{0.7}\text{Sr}_{0.3}\text{MnO}_3$ -glass composites, *Appl. Phys. Lett.*, 2001, **78**, 362-364.
6. Hueso, L.E., Rivas, J., Rivadulla, F. & Lopez-Quintela, M.A., Magnetoresistance in manganite/alumina nanocrystalline composites, *J. Appl. Phys.*, 2001, **89**, 1746-1750.
7. Das, D., Srivastava, C.M., Bahadur, D., Nigam, A.K. & Malik, S.K., Magnetic and electrical transport properties of $\text{La}_{0.67}\text{Ca}_{0.33}\text{MnO}_3(\text{LCMO}):\text{ZnO}$ composites, *J. Phys. : Condens. Matter*, 2004, **16**, 4089-4102.
8. Shlyakhtin, O.A., Shin, K.H. & Oh, Y.J., Enhancement of low field magnetoresistance by chemical interaction in bulk composites $\text{La}_{0.7}\text{Sr}_{0.3}\text{MnO}_3/\text{SrMeO}_3$ (Me = Ti, Zr), *J. Appl. Phys.*, 2002, **91**, 7403-7405.
9. Huang, B.X., Liu, Y.H., Zhang, R.Z., Yuan, X., Wang, C.J. & Mei, L.M., Low-field MR behaviour in $\text{La}_{0.67}\text{Ca}_{0.33}\text{MnO}_3/\text{ZrO}_2$ composite system, *J. Phys. D: Appl. Phys.*, 2003, **36**, 1923-1927.
10. JCPDS, Powder Diffraction File Database
11. Vertruyen, B., Rulmont, A., Cloots, R., Fagnard, J.-F., Ausloos, M., Vandriessche, I. & Hoste, S., Low-field magnetoresistance in $\text{La}_{0.7}\text{Ca}_{0.3}\text{MnO}_3$ manganite compounds prepared by the spray drying technique, *J. Mater. Sci.*, 2005, **40**, 117-122.
12. Dabrowski, B., Dybzinski, R., Bukowski, Z., Chmaissem, O. & Jorgensen, J.D., Oxygen content and structures of $\text{La}_{1-x}\text{Ca}_x\text{MnO}_{3+d}$ as a function of synthesis conditions, *J. Solid State Chem.*, 1999, **146**, 448-457.
13. McLachlan, D.S., Blaszkiewicz, M. & Newnham, R.E., Electrical resistivity of composites, *J. Am. Ceram. Soc.*, 1990, **73**, 2187-2203.
14. Ziese, M. & Sena, S.P., Anisotropic magnetoresistance of thin $\text{La}_{0.7}\text{Ca}_{0.3}\text{MnO}_3$ films, *J. Phys.: Condens. Matter*, 1998, **10**, 2727-2737.

Figure captions

Figure 1: Manganite volume fraction and crystallographic cell volume (Pnma space group) as a function of the manganese excess.

Figure 2: Electron micrograph of a polished cross-section of the Mn-100 sample.

Figure 3: Curie temperature (T_C) and resistive transition temperature (T_{IM}) as a function of Mn excess. Inset: Magnetization at 2T and 10 K as a function of Mn excess: comparison of experimental data (black symbols) with theoretical prediction (plain line).

Figure 4: 300 K electrical resistivity as a function of Mn excess. Inset: Normalised electrical resistance $R/R(0)$ as a function of applied magnetic field ($-0.15 \text{ T} < \mu_0 H < 0.15 \text{ T}$) for the sample Mn-633 at 77 K.

Figure 5: Normalised electrical resistance $R/R(0)$ as a function of applied magnetic field ($-2 \text{ T} < \mu_0 H < 2 \text{ T}$) for the sample Mn-633 at different temperatures.

Figure 1

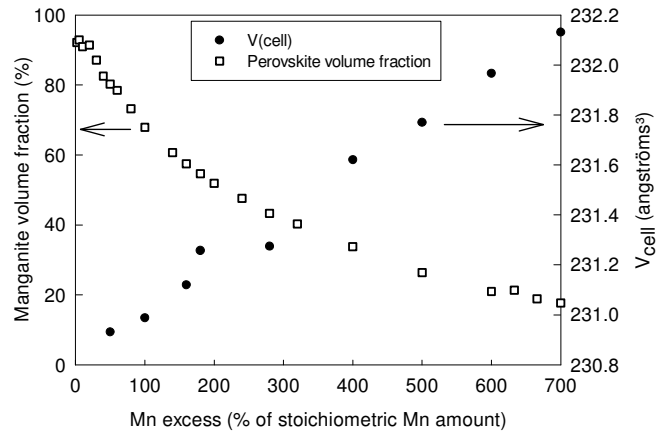


Figure 2 :

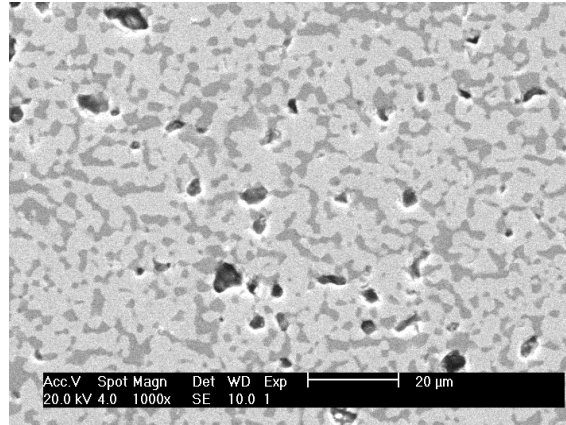


Figure 3

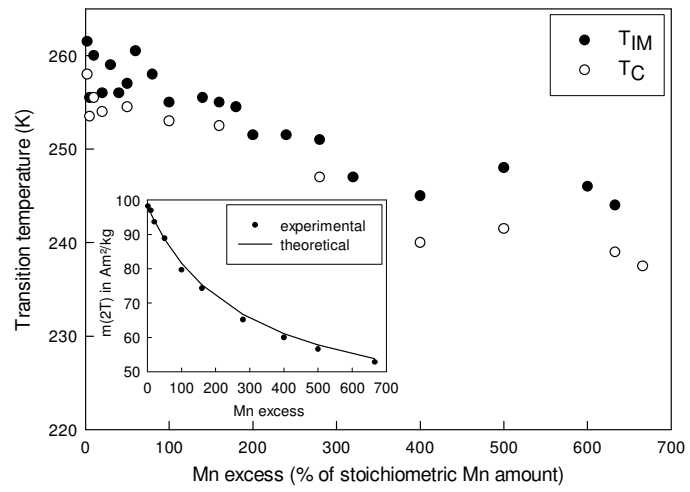


Figure 4 :

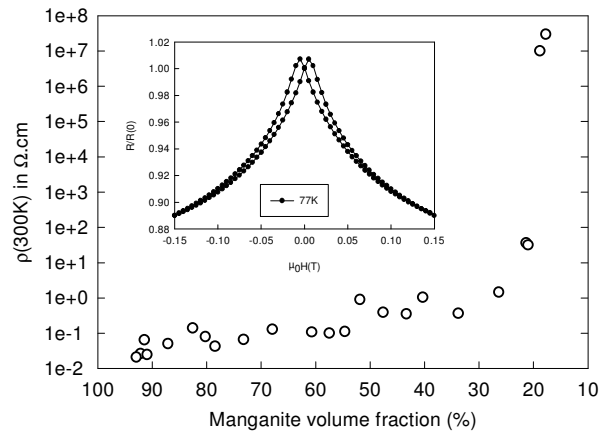


Figure 5 :

